A Sustainable Carbon Material from Kraft Black Liquor as Nickel-Based Electrocatalyst Support for Ethanol Electro-Oxidation

Gisele Amaral-Labat, E. Leal da Silva, A. Cuña, C. Malfatti, J. Marcuzzo, M. Baldan, A. Celzard, V. Fierro, G. Lenz E Silva

A sustainable carbon material from Kraft black liquor as nickel-based electrocatalyst support for ethanol electro-oxidation

G. Amaral-Labat[a,b*], E. Leal da Silva[c,d], A. Cuña[c], C. F. Malfatti[d], J. S. Marcuzzo[e], M.R. Baldan[b], A. Celzard[f], V. Fierro[f], G.F.B. Lenz e Silva[a]

[a]University of São Paulo, Department of Metallurgical and Materials Engineering PMT-USP, Avenida Mello Moraes, 2463-Cidade Universitária, CEP 05508-030, - São Paulo, SP – Brazil

[b] Associated Laboratory of Sensors, Nacional Institute of Space Research - INPE, 12227-010, São José dos Campos/SP, Brazil

[c]Area Fisicoquímica, DETEMA, Facultad de Química, Universidad de la República - Avenida General Flores 2124, CC 1157, Montevideo, 11800, Uruguay

[d]LAPEC/PPGE3M, Universidade Federal do Rio Grande do Sul, Av. Bento Gonçalves, 9500, setor 4, prédio 75, sala 232 - 91501-970 – Porto Alegre/RS, Brazil

[e]Federal Institute of São Paulo – IFSP, Campus São José dos Campos, Rod. Pres. Dutra, km 145, São José dos Campos, São Paulo, Brasil.

[f]Institut Jean Lamour - UMR Université de Lorraine – CNRS n°7198. ENSTIB, 27 rue Philippe Séguin, BP 21042, 88051 Épinal cedex 9, France

* Corresponding author. Phone number: +55 1130915494. E-mail address: gisele.amarallabat@gmail.com (Gisele Amaral-Labat)

Abstract

The present work deals with a new methodology to produce a sustainable carbon material through a simple synthetic route, and its performance as Ni-based electrocatalyst support. Such porous carbon was easily synthesized from the raw Kraft black liquor, a by-product rich in lignin, by chemical polymerization in alkaline medium with a nickel source and subsequent activation by CO_2. Nickel nanoparticles were homogeneously distributed in the samples, as revealed by STEM images. XPS analyses and BET method indicated the presence of Ni species in the synthesized material and a micro-mesoporous structure, respectively. The electrochemical characterization in NaOH and NaOH + ethanol solutions showed that the as-prepared material has the relevant potential to be applied as electrocatalyst for Ethanol Oxidation Reaction (EOR) in alkaline medium.

Keywords: Paper and pulp industry by-product, Kraft black liquor, Sustainable porous materials, Ni-based electrocatalyst, Ethanol electro-oxidation

Graphical abstract

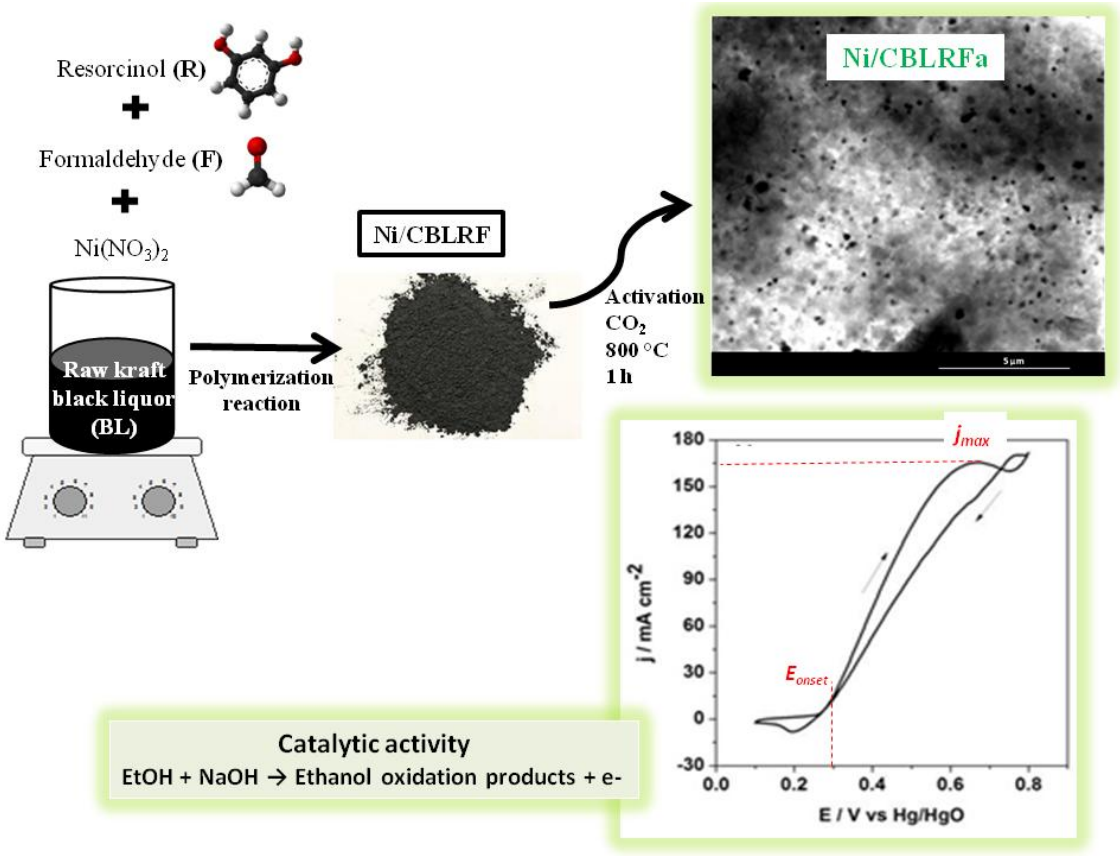

Statement of Novelty

This work is about the use of a paper and pulp industry by-product to produce a porous carbon material as catalyst support for ethanol electro-oxidation, aiming the use as active material in direct ethanol fuel cells electrodes. We showed a new methodology to produce a sustainable Ni-based electrocatalyst, using Kraft black liquor as raw material and a polymerization reaction followed by carbonization/activation steps. The produced material present good features for being used as electrocatalyst since the maximum ethanol oxidation current density is rather similar compared to those reported in the literature. However, is import to highlight that the developed material consists in a low-cost catalyst source deposited on a sustainable carbon support.

1. Introduction

The Kraft pulping process represents 90% of the world chemical pulp production [1]. It generates large amounts of liquid by-product, the production of 1 ton of pulp indeed leading to around 1 ton of black liquor [2]. Only in 2013, approximately 130 million tons of Kraft black liquor was generated worldwide [3]. Such residue is normally concentrated in evaporators for chemical reagents recovery, and then is marginally burnt in boilers for energy production [4,5]. Therefore, the amount of pulp produced is limited by the volume of the recovery boiler [5], and the excess of Kraft black liquor has no really relevant application on the market. At the same time, a strong trend towards a higher production of pulp is observed as a result of the growing demand, and also due to an environmental pressure in order to replace synthetic plastic products by biodegradable or papers ones. Given all this, in the recent years, different works have been carried out aimed at finding the best way to properly process and valorize the Kraft black liquor [6-8].

The Kraft liquor residue is substantially rich in lignin (35-45 wt. %) [4], but contains other components such as cellulose, hemicellulose, organic acids and extractives derived from wood, as well as sodium salts, sulfur compounds and inorganic matter added during the delignification process [9]. The huge amounts of available lignin in the liquor and its reactivity with formaldehyde [10] are attractive for using it in a number of applications. However, such byproduct is currently undervalued because of the expensive steps of purification to isolate the lignin, minimizing its viability for a large-scale use. For example, out of all kinds of lignin extracted worldwide in 2010, only 2% was used for the preparation of dispersants, adhesives and surfactants, or as antioxidant in plastics and rubbers [4].

Additionally, extraction and purification methodologies of lignin from black liquor are destructive and consequently modify the original polymer network of the macromolecule [11]. The isolation processes normally produce a less reactive lignin, since its chelation properties, associated to oxygenated functional groups, disable the most reactive sites. As a result, a more crosslinked macromolecule is obtained [12]. Furthermore, precipitation and purification steps require an additional use of chemicals (CO_2, HCl, H_2SO_4) [13], followed by extensive washing, making the process economically impracticable. Furthermore, lignin is already dissolved, and an additional use of alkalis for such purpose is avoided. Besides, the increased OH^-/H^+ of the final black liquor catalyze phenolic reactions with formaldehyde [14]. Finally, the possible remains of dissolved hemicelluloses and cellulose might also participate and assist the polymerization reaction, once those molecules also react with formaldehyde [15,16].

The production of bio-based porous materials from raw Kraft black liquor might be a motivating outlet for the paper industry. Firstly, the growing interest for the concept of sustainability has stimulated the use of wastes and by-products as alternative raw materials in new processes. Secondly, the materials produced from wastes might contain the largest amount of renewable and low-cost resources, thus representing an attractive alternative to the current market. Finally, the use of a fraction of black liquor in another process may allow an increase of pulp production without additional costs for the plant process [5,17].

On the other hand, direct ethanol fuel cells (DEFCs), based on ethanol oxidation reaction (EOR), constitute an alternative energy conversion system with very promising applications [18]. In this type of fuel cells, the EOR occurs at the fuel cell anode on the surface of certain electrocatalysts. Generally, the electrocatalysts for EOR consist in nanometer-sized metal or alloy particles deposited on an adequate support material [19].

Normally, the type of catalyst changes depending on the acidic / basic character of the reaction medium of EOR, leading to either acidic or alkaline DEFCs, respectively. A considerable attention has been paid to the preparation and characterization of electrocatalysts for EOR in alkaline medium, because the fuel oxidation and oxygen reduction reactions are faster than in acidic conditions [20-25]. Most of recent studies are focused on efficient but costly catalyst metals, i.e., based on Pd [25-29] and PdM alloys where M stands for Pt, Ni, Sn, Au, Ru, Cu and Ag [30-34].

From this point of view, much cheaper materials such as pure nickel [21,35] or nickel-based nanocomposites on different substrates [36-40] would be of high interest. The latter have indeed been successfully tested for ethanol electro-oxidation (EEO) in alkaline medium, although some optimizations are still needed to improve the catalytic performance and also to validate alternative methodologies of synthesis that would be both simpler and cheaper.

This work presents a new methodology to produce a sustainable porous carbon material from raw black liquor and its application as nickel catalyst support for ethanol oxidation reaction (EOR) in alkaline direct ethanol fuel cells (DEFCs). Structural and morphological analyses were performed using Scanning Transmission Electronic Microscopy (STEM), Energy Dispersive Spectroscopy (EDS), X-ray diffraction (DRX) and Thermogravimetric Analysis (TGA) techniques. The surface chemistry was evaluated by X-Ray Photoelectron Spectroscopy (XPS), and electrocatalytic performances were studied by electrochemical characterization.

2. Experimental section

2.1 Synthesis of lignin-based porous materials

The Kraft black liquor, kindly supplied by the company Suzano Papel & Celullose, was used as received. It is a weak black liquor from *Eucaliptus sp.* (hardwood) presenting a solid content from 15 to 18 wt. % and pH ~13 [41].

The density and the solid contents of the raw black liquor were accurately measured in triplicate by determination of volume and weight in pycnometry vials, and by gravimetric tests of samples weighed before and after drying at 105°C for 24 h, respectively. The pH of black liquor was measured at room temperature and finally the ash content of dried black liquor was also determined by the average of six samples. The samples were burnt in a muffle oven at 900°C for 2 hours. Firstly, an empty porcelain crucible was weighed and then about 0.5g of each sample was weighted into the same tarred porcelain crucible. At the end of the process, the samples were moved to a desiccator to cool down and reweighted. Ash content was also performed at 575°C following the ASTM E1755-01 standards [42].

Lignin-based porous materials were synthesized as explained below by polymerization of the raw black liquor in alkaline medium in the presence of resorcinol, formaldehyde and $Ni(NO_3)_2.6H_2O$. Table 1 shows the formulation that was used, and the function of each component.

Table 1 Formulation of polymerized black liquor.

Component	Function	Quantity (g)
Black liquor (BL)	Main raw material	100.0
Resorcinol (R)	Co-monomer	15.0
Formaldehyde (37 wt. % aqueous solution) (F)	Crosslinker	44.0
$Ni(NO_3)_2.6H_2O$	Catalyst source	7.4

In a typical experiment, 15g of resorcinol was dissolved in 100 g of raw black liquor and was continuously stirred to facilitate the dissolution. Then, $Ni(NO_3)_2.6H_2O$ was introduced into the solution, followed by a 37 wt. % aqueous solution of formaldehyde (44g). The blend was stirred at room temperature until complete dissolution of solids and achieving a homogeneous liquid. Finally, the sample was left to harden, cure and dry in room conditions for 5 days. The obtained sample (Polymerized BL) was finally washed with deionized water until the pH of the rinse remained constant and neutral. Afterwards the polymerized BL was dried at 105°C for 24h before carbonization, generating a dark brown powder.

2.2 Preparation of the porous carbon material

The sustainable carbon material, a fine powder with particles lesser than 100 μm, was obtained by pyrolysis and subsequent physical activation of Polymerized BL with CO_2. For that purpose, Polymerized BL was heated at 5 °C min^{-1} from room temperature to 800°C under N_2 flow (99.998% pure, 200 mL min^{-1}). Then, the gas flow was switched to CO_2 (99.98% pure, 200 mL min^{-1}) and maintained at 800°C. After 1 hour, the oven was cooled down to room temperature under argon flow. The resultants carbons material was termed Ni/CBLRFa, where Ni, C, BL, R, F, and a stand for nickel, carbon, black liquor, resorcinol, formaldehyde, and activated, respectively. All the aforementioned thermal treatments were carried out in a horizontal Carbolite (CTF 12/75) tubular furnace.

2.3 Characterization methods

Polymerized black liquor was characterized as explained below. For the sake of comparison, lignin was also extracted from the same Kraft black liquor with gaseous CO_2, and then purified with solutions of H_2SO_4 according to the method described elsewhere [13].

Differences of functional groups between purified lignin, resorcinol, and polymerized black liquor were evaluated by FTIR spectroscopy, using a Nicolet IDS spectrophotometer equipped with a Thermo Scientific ATR-Diamond. Spectra were acquired in the range of wavenumbers of 600-4000 cm^{-1}, by averaging 20 scans at a resolution of 4 cm^{-1}.

The main chemical elements of the final material were observed and quantified by the EDX accessory of a FEI-INSPEC scanning electron microscope, using EDAX and TEAM software.

Size and morphology of nickel particles were evaluated by scanning transmission electronic microscopy (STEM module /FEG – INSPECT F50). For that purpose, the activated carbon sample was ground in ethanol and dispersed in an ultrasound bath apparatus, and then a few drops of the resultant suspension were collected on the grid of a sample holder. The histogram of nickel distribution was determined by measuring more than 200 nanoparticles.

The Ni metal loading in the electrocatalyst was estimated by Microwave Inducted Plasma Atomic Emission Spectroscopy (MP-AES) using an Agilent MPAES 4210 equipment. Sample was prepared by dissolving a known amount of Ni/CBLRFa in HNO_3, followed by several dilutions. All solutions (sample, stock solutions for calibration curve and control) presented a final concentration of 0.05 mol L^{-1} HNO_3.

The textural properties of the Ni/CBLRFa sample, previously outgassed for 15 h at 150 ºC and 10^{-2} Pa, were obtained from N_2 adsorption/desorption isotherms at 77 K using a Beckman Coulter SA 3100 equipment. Isotherm parameters as surface area, S_{BET} and micropores volume, V_{DR}, (region <2 nm), were determined using Brunauer-Emmet-Teller (BET) [43] and Dubinin–Radushkevich [44] calculation methods, respectively. The volume of mesopores, V_{meso}, (region 2-50 nm) was calculated as $V_{meso} = V_{0.99} - V_{DR}$. $V_{0.99}$ is the volume of liquid nitrogen corresponding to the amount adsorbed at a relative pressure $P/P_0 = 0.99$ [45]. Pore-size distribution was calculated using the density functional theory DFT method [46].

TGA of dried BL, polymerized BL and activated sample (Ni/CBLRFa) were performed using a Shimadzu TG-50 thermobalance. The BL and polymerized BL was analyzed under argon atmosphere and the Ni/CBLRFa in air and nitrogen atmosphere. All analyses were performed from 25 to 900°C, at a heating rate of 10°C min^{-1}, using samples of weight 8.0 – 10.0 mg placed in a platinum crucible.

XRD analyses were performed with a Rigaku Ultima IV diffractometer, using the Cu $K_{\alpha 1}$ radiation (wavelength 1.54 Å). The XPS measurements were carried out with a Kratos Axis Ultra spectrometer using a monochromatized Al-K_α radiation source (1486.5 eV) operated at (150 W) 15 kV. Survey scans were collected from 0 to 1200 eV with 160 eV pass energy and step size of 1 eV, in order to identify the elements present on the surface, and pass energy of 40 eV was applied for high-resolution scans of specific atomic peaks.

The electrochemical behavior of the Ni/CBLRFa electrocatalyst was performed at room temperature in a standard three-electrode cell, using a platinum wire as counter-electrode, connected to an AUTOLAB PGSTAT 302N potentiostat/galvanostat. All the potentials were measured with respect to Hg/HgO reference electrode. A graphite disk was used as working electrode (geometric area of 0.29 cm^2) with 1.6 mg of the studied electrocatalyst. The preparation of this electrode was carried out by the addition of 255 μL of an ultrasonic homogenized (30 min) electrocatalyst powder suspension. This suspension was prepared with 12.7 mg of the sample, 25 μL of Nafion® (5 wt. %, Sigma-Aldrich) and 2.0 mL of ethanol (Merck). Prior to analysis, the electrode was dried in an oven at 25 °C for 24 h.

The cyclic voltammetry experiments were performed in a 1.0 mol L^{-1} NaOH solution and in a 1.0 mol L^{-1} ethanol + 1.0 mol L^{-1} NaOH solution, with a scan rate of 20 mV s^{-1} in a potential range from 0.1 to 0.8 V *vs.* Hg/HgO electrode. Chronoamperometry experiments were performed using 1.0 mol L^{-1} ethanol + 1.0 mol L^{-1} NaOH solution at 0.5 V over 60 min. For a comparison purpose, a chronoamperometry experiment was carried out for a Pd/Vulcan electrocatalyst. This last sample was prepared as described elsewhere [47]. All the solutions

were de-aerated by N_2 purging during 10 min prior to the measurements. In order to avoid the presence of oxygen in the medium, a continuous stream of nitrogen was forced to bubble inside the solution during all the electrochemical experiments.

3. Results and Discussion

3.1 Black liquor characterization and polymerization

The residual liquor from the Kraft pulping process is a dark liquid with a characteristic strong odor and a complex composition based on different compounds [9]. However, lignin is the major component [4] and the polymerization reactions carried out in the present work are mainly based on such molecule. However, since lignin is based on highly substituted aromatic rings presenting a significant steric hindrance, its reactivity is rather low. Therefore resorcinol, which bears two reactive free sites, and being thus far more reactive, was used as co-monomer for polymerizing black liquor. The whole was crosslinked with formaldehyde, thereby leading to the precursor of the present carbon material.

Black liquor residue presented a percentage of solids of 15 wt. %, a pH of 12.5 and a density of 1.09 g/cm^3 at a temperature of 25°C. TGA of the dried black liquor is presented in Fig. 1, showing a significant amount of mass retained at 900°C, containing a relevant quantity of organic material, as indicated by the ash content (35.0 % and 39.0% of inorganics at 900°C and 575°C, respectively). The value of ash content calculated at 575°C is in agreement with results reported by Gea (39.11%) [48]. Such organic material, especially lignin, might produce a final material with high carbon content.

DTG curve of raw Kraft black liquor showed mass loss rate with four main maximal degradation peaks (DTG_{max}) (Figure 1a). The first thermal degradation at 96°C is attributed to moisture of black liquor, while the decomposition region from 200°C to 520°C, presenting peaks centered at 280°C and 426°C, might be related to degradation of main organic compounds on the black liquor as hemicelluloses (200-260°C), aliphatic carboxylic acids (200-300°C), lignin (280-500°C) and holocellulose (280°C) [48,49], through several decomposition reactions, releasing gases as phenol molecules, hydrocarbons, CO and CO_2 [50,51]. The last DTG_{max} (714°C) correspond to the decomposition of inorganic matter, i.e., volatilization of alkaline metals [48].

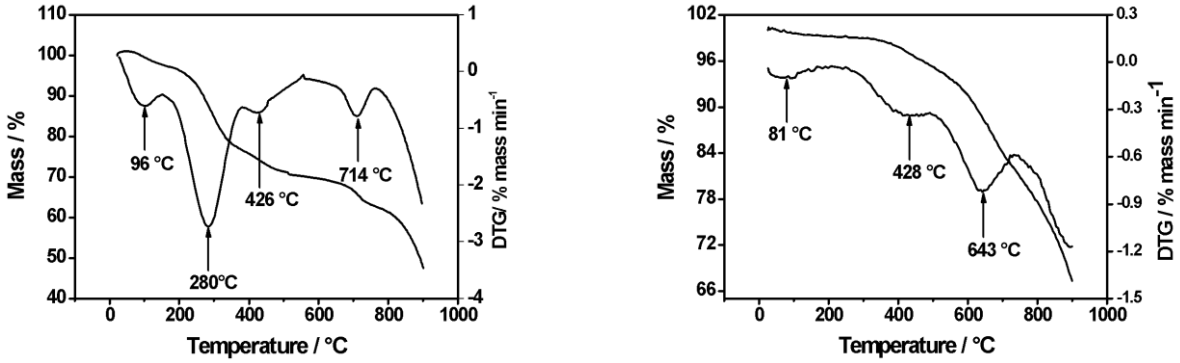

Fig. 1 TGA/DTG curves of (a) raw, dried, BL and (b) polymerized BL under argon.

Lignin and resorcinol readily polymerize in the presence of formaldehyde in alkaline medium. The first step is the formation of methylol groups (derived from formaldehyde) on lignin, and then the modified lignin fragments react with each other or with resorcinol to produce a crosslinked polymer [52]. The crosslinking reaction was evaluated by DTG curve of polymerized black liquor (Figure 1b) and FTIR by observing the main differences between the raw materials on one hand, i.e., pure lignin and resorcinol, and the polymerized black liquor on the other hand, see Fig. 2a.

Thermal degradation of polymerized BL (Figure 1b) showed a moisture content at 81°C and a decomposition around 428 °C due to rupture of weak bonds of crosslinked lignin in the final resin [53]. The thermal degradation at 280°C was not found in the polymerized BL, suggesting that the organic matter, with different nature of lignin molecules, are also composing the formed polymer network, since these compounds are normally degraded at temperatures below 350°C, as mentioned above. Finally, the DTG_{max} at 643 °C is probably associated to the carbothermal reduction of alkaline compounds [48] or NiO [54].

The spectrum of purified lignin showed a peak at 1726 cm^{-1}, attributed to C=O stretching from unconjugated ketone, carbonyl and ester groups [55,56], was no more visible in the spectrum of the polymerized BL, indicating a probable reaction with formaldehyde and/or resorcinol. Finally, the full range of bands from 1600 to 830 cm^{-1} present on the Polymerized BL are contributions of raw lignin and resorcinol to the spectrum.

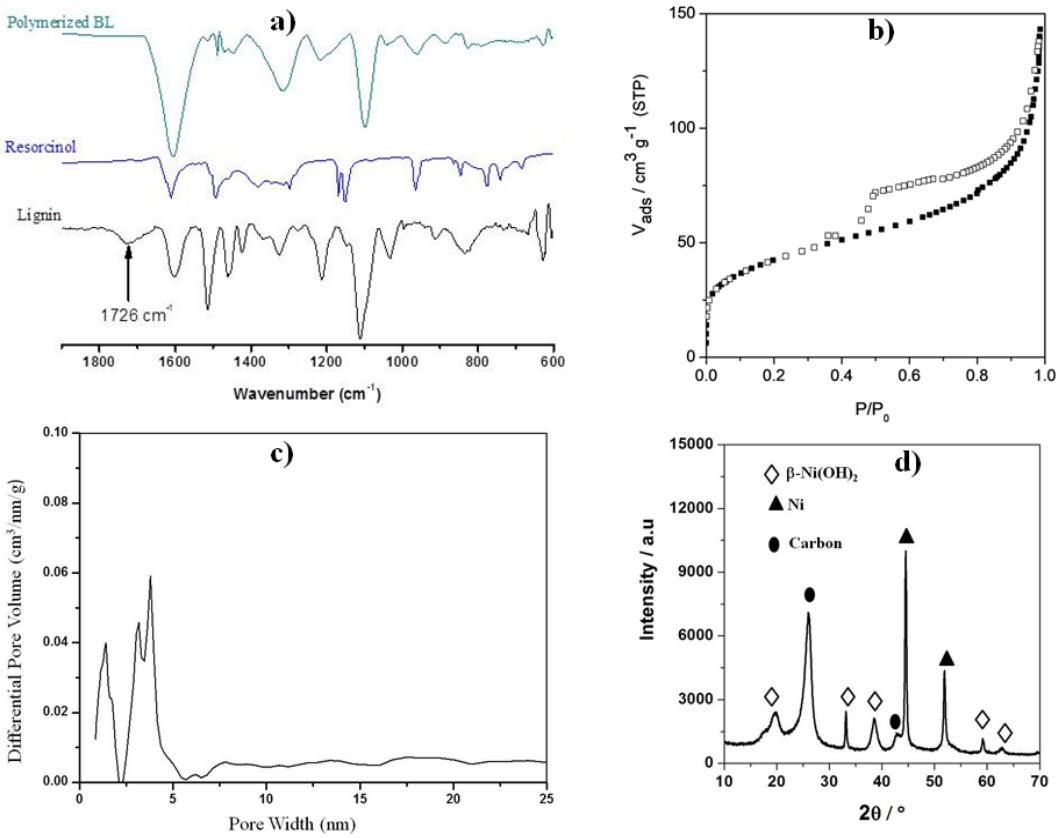

Fig. 2 a) FTIR spectra of purified lignin, resorcinol and polymerized black liquor. b) N_2 adsorption-desorption isotherm (full and open symbols, respectively) of the Ni/CBLRFa sample. c) Pore size distribution of the Ni/CBLRFa sample. d) X-ray diffraction pattern of the Ni/CBLRFa sample.

3.2 Characteristics of the carbon material

Fig. 2b shows the N_2 adsorption/desorption isotherm of the Ni/CBLRFa electrocatalyst. Sample curves show a combination of type I and IV isotherms (micro–mesoporous) [57], presenting a hysteresis, usually associate with capillary condensation in mesopores. Those parameters also indicate adsorption occurs on an open surface at high relative pressures [58]. Hysteresis loop for the samples is classified as type H3 and it is characteristic of slit-shaped pores [59]. The S_{BET} (151 $m^2 g^{-1}$) of the sustainable electrocatalytic system (carbon based nickel) is smaller than other biomass derived carbons [60] but is slightly smaller to the values reported for the commercial Vulcan XC72 carbon (200 m^2 g^{-1}) commonly used as support of electrocatalysts for fuel cells [61,62]. The material presented a high proportion of micropores (90%) and an important mesoporosity (9%), that might provide an effective access for the electrolyte solution to the electrocatalyst.

Table 2 Textural parameters of Ni/CBLRFa sample

S_{BET} (m^2/g)	V_{DR} ($cm^3\ g^{-1}$)	V_{meso} ($cm^3\ g^{-1}$)	$V_{DR}/V_{0.99}$ (%)	$V_{meso}/V_{0.99}$ (%)
151	0.21	0.02	91	9

The XRD pattern given in Fig. 2d for Ni/CBLRFa shows peaks at 44.5°and 51.8° corresponding to the (111) and (200) reflections of crystalline Ni, respectively [63,64]. Peaks at 19.9°, 33.2°, 38.4°, and 63.0 also reveals the planes (100), (011), (110), and (111), respectively, associated to β-$Ni(OH)_2$ [65]. Furthermore, the peaks at 26° and 42.4° is related to the (002) and (100) plane of graphitic structures [66] from carbon matrix.

Fig. 3 shows the XPS survey and the corresponding high-resolution C1s, O1s and Ni2p XPS spectrum. Various surface moieties involving carbon, oxygen and nickel were found at the surface of the material, as shown by the XPS survey scan presented in Fig. 3a.

The carbon C1s XPS spectrum, presented in Fig. 3b, shows oxidized species typically associated with activated carbons at 800°C [67]. As usually reported in the carbon literature, binding energies around 284.6–285.1 eV are related to graphitic (sp2) carbon. C-O is observed at 286.3–287.0 eV and may indicate alcohol or ether groups. Carbonyl and/or quinone groups (C=O) corresponding to 287.5–288.1 eV, as COO (289.3–290.0 eV) indicate carboxyl or ester groups, while (O-C=O) may be associated to energies around 288.6 eV. The energies around 291.2–292.1 eV correspond to carbon satellite peaks [67-69]. The peaks above 292.0 eV might be related to overlap spectra, in this case K2p.

The high-resolution O1s XPS spectrum is presented in Fig. 3c and was fitted by considering four peaks normally found in the carbon literature. The energy ranging at 530.4–530.8 eV for (C=O and OH species) [70] and 532.4–533.1 eV for (C-O bond in C-OH and/or C-O-C groups) [71] and the energy around 533 eV is associated to H-C-O bonding.

As presented before, nickel is present in the bulk material as Ni° and $Ni(OH)_2$ (see Fig. 2d), but on the surface a different Ni compound could be found. The Ni2p spectra shows peaks at 857.9 and 856.2 assigned to NiOOH and $Ni(OH)_2$, respectively (Fig. 3d) [72]. Those species are important on the electrochemical reactions involved on the ethanol oxidation.

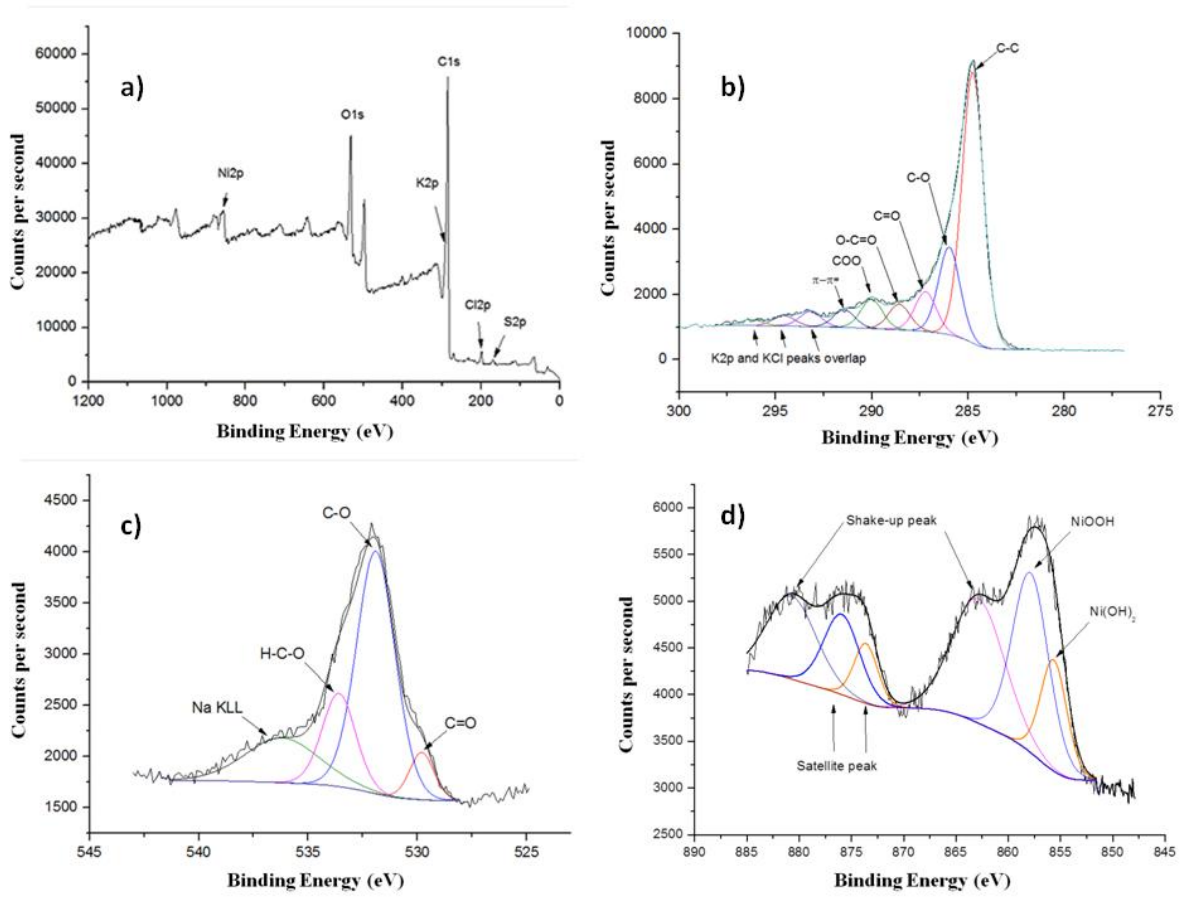

Fig. 3. XPS survey scan of Ni/CBLRFa sample (a) and the corresponding high-resolution C1s (b), O1s (c) and Ni2p (d) XPS spectrum.

STEM micrographs of the synthesized Ni/CBLRFa (Fig. 4(a-c)) demonstrated the existence particles homogeneously distributed all over the carbon support, having a broad size distribution and an average size close to 130 nm (Fig. 4d). The EDX spectra of selected area (Fig. 5) evidenced the elements expected to be present in the material: carbon, oxygen and nickel, as well as the impurities recovered from the delignification process: sulfur, potassium and sodium. However, the latter were not detectable by XRD and XPS, suggesting that most of observed particles correspond to Ni^{o} and β-$Ni(OH)_2$. The formation of these particles could be explained as follows: During the polymerization reaction of Kraft BL, an in-situ precipitation of NiO and β-$Ni(OH)_2$ particles, on the resulting polymer, is prone to occur due to the presence of nickel nitrate in the reactional medium [73]. Concurrently, during the carbonization/activation step, a carbonaceous matrix is developed and the following processes might occur (i) the formation of Ni particles through the thermal dissociation mechanism [35,74] (ii) and/or the oxide reduction through intermediates gases [35].

On the other hand, the Ni metal loading in the Ni/CBLRFa sample determined by MP-AES analysis was (8.3 ± 0.4) wt. %. This value is in the same order of commercial Pt or Pd based electrocatalysts.

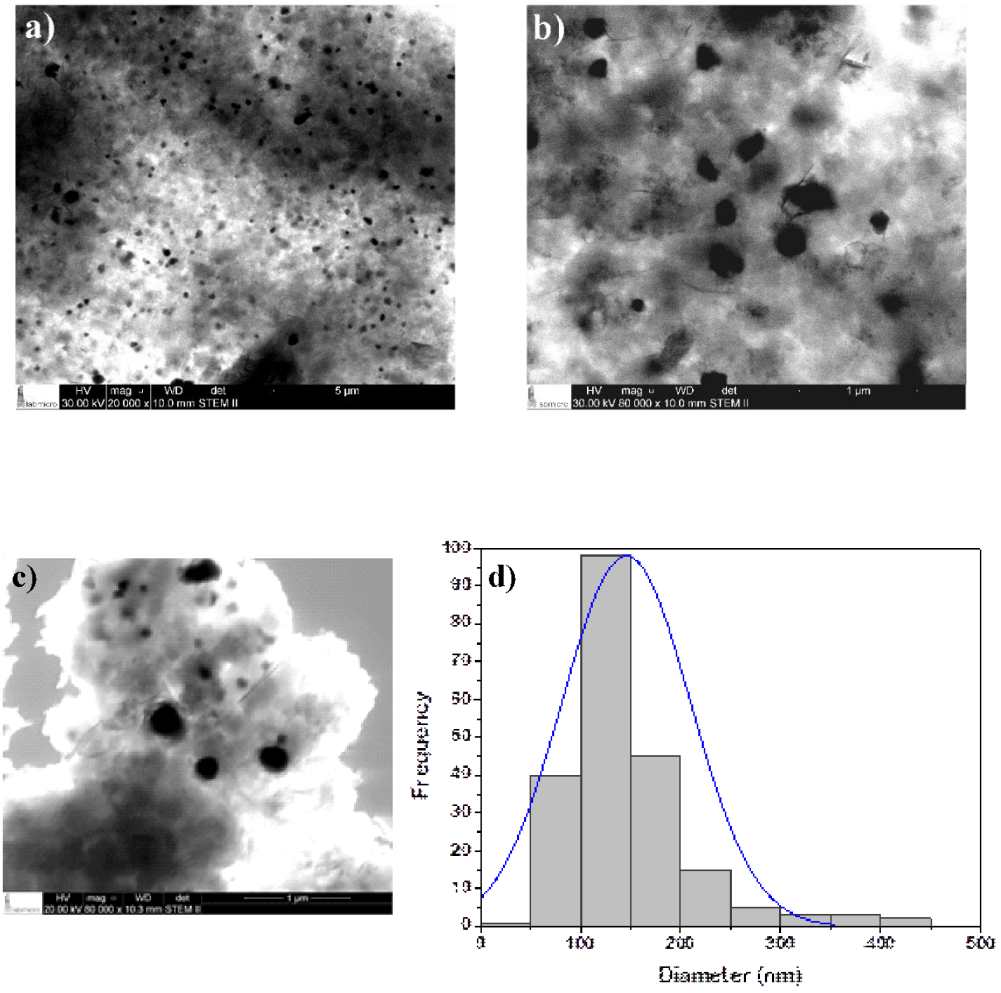

Fig. 4 STEM images of Ni/CBLRFa (a-c) and corresponding particle size distribution (d).

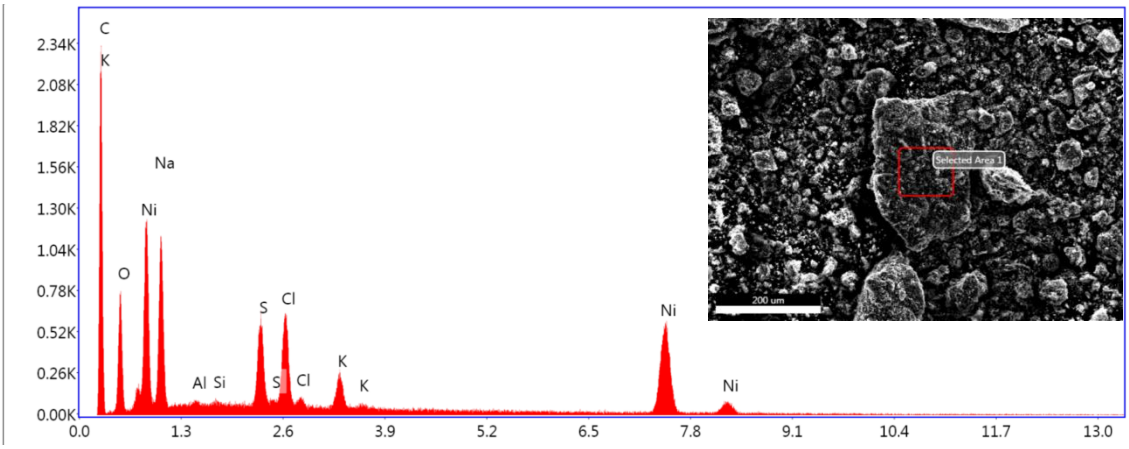

Fig. 5 EDX analysis of the sample Ni/CBLRFa (indicated by the red square on the right image).

Fig. 6a shows the TGA and DTG curves obtained for the Ni/CBLRFa sample in air atmosphere. During heat treatment in air, the activated sample showed an expected weight loss corresponding to the degradation reaction of the carbon material with a DTG peak at 496 ºC, while under inert atmosphere (Fig. 6b) such decomposition is observed at 514 ºC. Furthermore, above ~250 ºC (Fig. 6a), the metallic Ni particles should oxidize leading to a weight increase [35,75], but by far compensated by the weight loss of the carbon being oxidized in air. Finally, in both atmospheres, a DTG peak is observed at ~310 ºC, probably associated to the mass loss of the NiO formation from β-$Ni(OH)_2$ nanoparticles present in the sample [74].

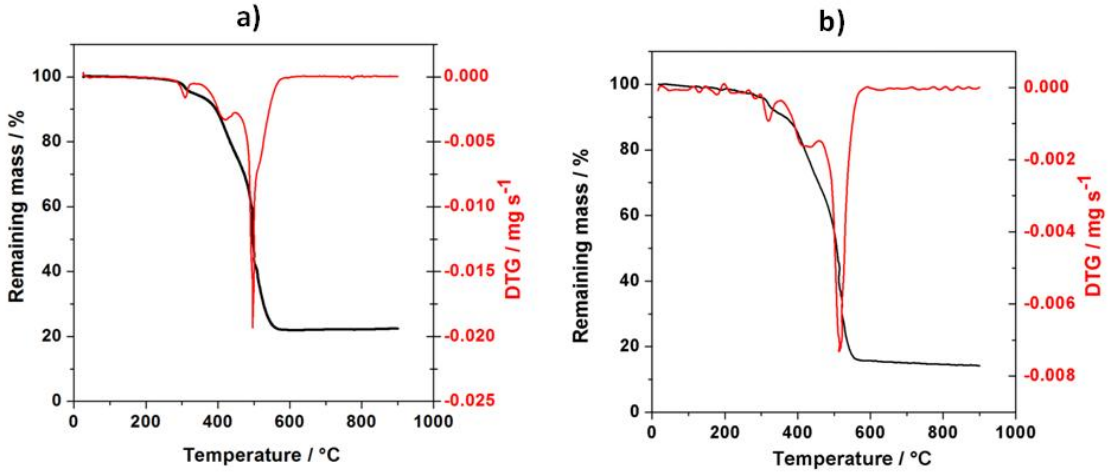

Fig. 6 TGA and DTG curves of activated sample in air (a) and inert (b) atmosphere.

3.3 Electrochemical performances in alkaline medium

The sample Ni/CBLRFa was evaluated as electrocatalyst for EOR in alkaline medium. Fig. 7 (curve A) presents the corresponding cyclic voltammogram in 1.0 mol L^{-1} NaOH solution. An anodic peak at 0.35 V and a cathodic peak at 0.14 V *vs.* Hg/HgO are clearly observed. These redox couple reactions have been linked to the reversible oxidation of NiO(OH) [21,76] according to:

$$Ni(OH)_2 + OH^- \leftrightarrows NiO(OH) + H_2O + e^- \quad (1)$$

The nickel oxyhydroxide might participate as active chemical species in the oxidation of organic compounds such as methanol or ethanol on nickel catalyst [21,35,76]. Therefore, nickel oxyhydroxide can participate to the EOR on the Ni/CBLRFa electrocatalyst by the following reaction:

$$NiO(OH) + \text{ethanol} \rightarrow Ni(OH)_2 + \text{ethanol oxidation products} \quad (2)$$

Fig. 7 (curve B) shows the voltammogram obtained for the Ni/CBLRFa sample in 0.1 mol L^{-1} NaOH + 1.0 mol L^{-1} ethanol solution. The increase in the current density (*j*) from 0.30 V *vs.* Hg/HgO could be related to the

catalytic activity of the sample in relation to EOR and the mentioned potential corresponds to the onset potential (E_{onset}) of the EOR on the electrocatalyst. This potential is very close to the formation potential of NiO(OH) (0.35 V *vs.* Hg/HgO), confirming that the species NiO(OH) is involved in the EOR mechanism. Comparing the *j* value of the curves A and B at 0.5 V it is clearly seen that the *j* of the curve with ethanol is approximately eight times larger than without ethanol indicating a good electrocatalytic behavior. On the other hand, at higher potentials (above 0.7 V vs. Hg/HgO), j values of the curve A increase, and, those high currents observed in the ethanol-free solution can be related to the Ni oxidation. Furthermore, in the presence of ethanol, the EOR should proceed in parallel with the Ni oxidation, probably until the Ni nanoparticles surface gets passivated.

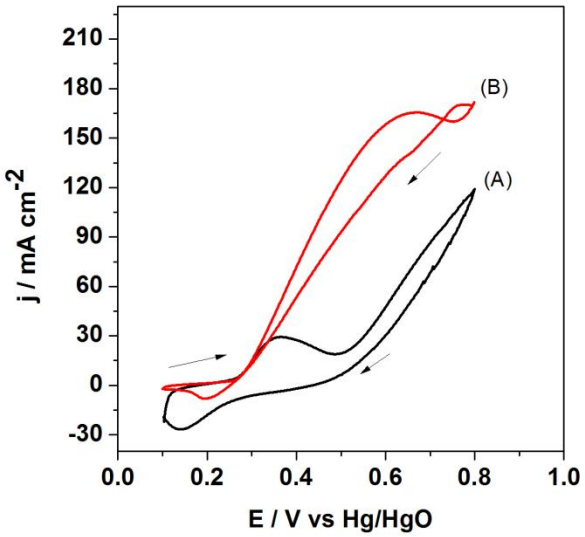

Fig. 7 (A) Cyclic voltammograms of the Ni/CBLRFa sample at a scan rate of 20 mV s^{-1} and 25°C in 1.0 mol L^{-1} NaOH; (B) Same as (A) but in a solution of 1.0 mol L^{-1} NaOH + 1.0 mol L^{-1} ethanol.

From the forward scan of the curve B, a peak current density (j_{max}) of 165 mA cm^{-2} is obtained at the potential (E_{max}) of 0.66 V *vs.* Hg/HgO. This j_{max} value is rather high or similar compared to those reported in the literature (see Table 3). For this comparison it is important to note that only j_{max} values obtained at the same voltammetry scan rate should be compared. However, a relative and semi-quantitative comparison can be made taking into account that for an irreversible reaction the corresponding peak current is proportional to the square root of scan rate [77]. On the other hand, with some exceptions, the E_{max} value of the analyzed sample is higher than that reported. Regarding the latter, is important to remember that from the DEFCs application point of view, E_{max} is expected to be as low as possible. Thus, future work should improve the material in this point. Considering the electrocatalyst load mass in the working electrode (1.6 mg) and the Ni metal loading in the electrocatalyst (8.3 wt. %), the calculated specific j_{max} values are 30 mA mg^{-1} (referred to the total mass) and 362.5 mA mg^{-1}Ni. These

values are in the same order or higher of other previous reported values for Ni [35] and Pd [23,47] based electrocatalysts.

Table 3 Electrocatalytic performance of different EOR electrocatalysts studied in a 1.0 mol L^{-1} EtOH alkaline solution.

Catalyst material	Scan rate ($mV\ s^{-1}$)	j_{max} ($mA\ cm^{-2}$)	E_{max} (V)	Reference
Ni/CBLRFa	20	165	0.66 *vs.* Hg/HgO	This work
Ni/aHC	50	45	0.70 *vs.* Hg/HgO	[35]
Ni hollow spheres	5	17	-0.15 *vs.* Hg/HgO	[64]
$NiCo_2O_4$/GCE	20	46	0.67V vs. Hg/HgO	[78]
Pt/C	10	45	0.15 V *vs.* Hg/HgO	[71]
NiPt/C	10	70	0.10 V *vs.* Hg/HgO	[71]
Pd/V	10	100	0.11 V *vs.* Hg/HgO	[47]
Pd/C-HNO_3	50	30	0.97 V vs. Hg/HgO	[79]
Pd_3Ni_3/C	50	217	-0.01 V *vs.* Hg/HgO	[80]
Pt-Ru/C	25	100	0.13 V *vs.* Hg/HgO	[81]

Fig. 8 shows the chronoamperometric curve for EOR on Ni/CBLRFa sample obtained by polarization at 0.5 V *vs.* Hg/HgO for 60 min compared with a Pd/Vulcan electrocatalyst. The prepared sample presents a constant density current (56 $mA\ cm^{-2}$) at least for the first 60 minutes, showing a similar stability behavior of a Pd/Vulcan electrocatalyst. Therefore, these results cannot guarantee its stability in a commercial application, once stability studies should ideally be performed over 24 h, but suggest a good candidate on a larger scale.

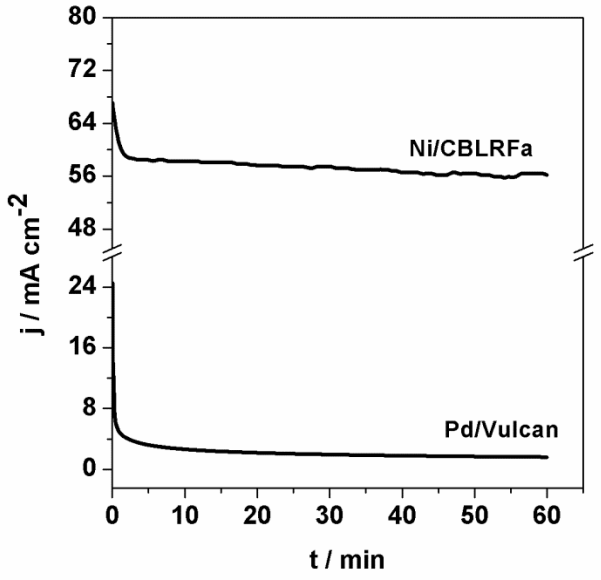

Fig. 8 Chronoamperometry curves of Ni/CBLRFa and Pd/Vulcan at 0.5 V in a solution of 1.0 mol L^{-1} NaOH + 1.0 mol L^{-1} ethanol.

The newly developed material proposed in this work is prepared from the raw BL by using a nickel as a non-noble and cheap catalyst. As can be seen in the *Supplementary Material*, the estimated production cost (only

based on the chemicals prices) of synthesized electrocatalyst is about 3 EUR/g, suggesting that the prepared sample could be price competitive with other commercial electrocatalysts, since the reactants has a high impact on the final price of the product, as already observed for other carbon material [82]. Obviously, to make a more accurate cost calculation, it would be necessary to consider other costs, e.g. energy, gases, manpower, among others. The main commercial electrocatalysts, based in noble metals, are the Pt/C (10 wt. % Pt) and Pd/C (10 wt. % Pd), and cost 16.1 EUR/g (Sigma-Aldrich, 205958-50G) and 5.7 EUR/g (Sigma-Aldrich, 205699-250G) respectively.

4. Conclusions

A new methodology to produce highly sustainable catalytic system for ethanol fuel cells was explored through the valorization of a liquid by-product from the Kraft pulping process. The main explored parameters were: (i) the integral use of the by-product for production of bio-based porous carbon material with a great amount of renewable and cheap by-product representing an attractive to the social, energetic, economic and environmental issues; (ii) the use of a cheap catalyst metal as nickel on a sustainable porous matrix support (iii) the use of ethanol instead of methanol.

The methodology proposes the polymerization reaction of the raw Kraft black liquor in alkaline medium performed at simple ambient conditions. Polymerization and activation steps of the material showed efficiency in the production of nickel based electrocatalyst supported on a sustainable porous carbon material, as demonstrated by XRD analysis and STEM images. The presence of NiO(OH) and $Ni(OH)_2$ could also be confirmed by the XPS analysis.

Electrochemical characterization showed that the material has a comparable performance for ethanol electrooxidation in alkaline medium with an electrocatalyst based in costly metals. Furthermore, the material also presented favorable electrocatalytic stability.

Conflicts of interest: The authors declare that they have no conflict of interest.

Acknowledgements: The authors are especially grateful to PhD. Mariela Pistón- Analytical Chemistry, Grupo de Análisis de Elementos Traza y Desarrollo de Estrategias Simples para Preparación de Muestras (GATPREM), Facultad de Química, Universidad de la República, Montevideo, Uruguay for the determination of Ni.

Funding: This study was supported in part by the Coordenação de Aperfeiçoamento de Pessoal de Nível Superior - Brasil (CAPES). E. Leal da Silva thanks the Uruguayan Comisión Académica de Posgrado (CAP)-Udelar for the Postdoctoral Fellowship (2018-2020).

References

[1] Azadi, P., Inderwildi, O.R., Farnood, R., King, D.A.: Liquid fuels, hydrogen and chemicals from lignin: A critical review. Renew. Sustainable Energy Rev. 21, 506-523 (2013).

[2] Mesfun, S., Lundgren, J., Grip, C.E., Toffolo, A., Nilsson, R.L.K., Rova, U.: Black liquor fractionation for biofuels production – A techno-economic assessment. Bioresour. Technol. 166, 508–517 (2014).

[3] Gouveia, S.L., Fernández-Costas, C., Sanromán, M.A., Moldes, D.: Polymerization of Kraft lignin from black liquors by laccase from Myceliophthora thermophila: Effect of operational conditions and black liquor origin. Bioresour. Technol. 131, 288-94 (2013).

[4] Laurichesse, S., Avérous L.: Chemical modification of lignins: Towards biobased polymers. Prog. Polym. Sci. 39, 1266-1290 (2014).

[5] Diehl, B.G., Brown, N. R., Frantz, C.W., Lumadue, M.R., Cannon, F.: Effects of pyrolysis temperature on the chemical composition of refined softwood and hardwood lignins. Carbon 60, 531-537 (2013).

[6] Xu, G., Yan, G. & Yang, J. An Integrated Green Process for Beneficial Utilization of Pulping Black Liquor. Waste Biomass Valor 4, 497–502 (2013). https://doi-org.proxy.timbo.org.uy/10.1007/s12649-012-9177-8

[7] Delgado, N., Ysambertt, F., Chávez, G. et al. Valorization of Kraft Lignin of Different Molecular Weights as Surfactant Agent for the Oil Industry. Waste Biomass Valor 10, 3383–3395 (2019). https://doi-org.proxy.timbo.org.uy/10.1007/s12649-018-0352-4.

[8] Domínguez-Robles, J., Palenzuela, M.V., Sánchez, R. et al. Coagulation–Flocculation as an Alternative Way to Reduce the Toxicity of the Black Liquor from the Paper Industry: Thermal Valorization of the Solid Biomass Recovered. Waste Biomass Valor (2019). https://doi-org.proxy.timbo.org.uy/10.1007/s12649-019-00795-7.

[9] Mänttäri, M., Lahti, J., Hatakka, H., Louhi-Kultanen, M., Kallioinen, M.: Separation phenomena in UF and NF in the recovery of organic acids from kraft black liquor. J. Membr. Sci. 49, 84-91 (2015).

[10] Pizzi A.: Types, processing and properties of bioadhesives for wood and fibers. In: Keith Waldron and Sarah Whitworth (Eds.), Advances in biorefineries: Biomass and waste supply chain exploitation, pp. 736-770. Woodhead Publishing Ltd, Cambridge (2014).

[11] Vazquez, G., Antorrena, G., Gonzalez, J., Freire, S.: The influencing of pulping conditions on the structure of acetosolv eucalyptus lignins. J. Wood Chem. Technol. 17, 147–162 (1997).

[12] Amaral-Labat, G.A., Gonçalves, A.R.: Oxidation in Acidic Medium of Lignins from Agricultural Residues. Appl. Biochem. Biotechnol. 148, 151-161 (2008).

[13] Bertaud, F., Tapin-Lingua, S., Pizzi, A., Navarrete, P., Petit-Conil, M.: Development of green adhesives for fibreboard manufacturing, using tannins and lignin from pulp mill residues. Cell Chem. Technol. 46, 449-455 (2012).

[14] Job, N., Pirard, R., Marien, J., Pirard. J.P.: Porous carbon xerogels with texture tailored by pH control during sol-gel process. Carbon 42, 619-628 (2004).

[15] Marsh, J.T.: Cellulose and Formaldehyde. J. Soc. Dyers Colour. 75, 244–252 (1959).

[16] Park, H., Park, K., Shalaby, W.S.W.: Biodegradable Hydrogels for Drug Delivery, CRC Press, Technomic, Switzerland (1993).

[17] Mirasol, J.R., Cordero, T., Rodriguez J.J.: Preparation and characterization of activated caibons from eucalyptus krafi-lignin. Carbon 31, 87-95 (1993).

[18] Dillon, R., Srinivasan, S., Aricò, A.S., Antonucci, V.: International activities in DMFC R&D: status of technologies and potential applications. J. Power Sources 127, 112–126 (2004).

[19] Antolini, E.: Carbon supports for low-temperature fuel cell catalysts. Appl. Catal., B 88, 1–24 (2009).

[20] Godoi, D.R.M., Villullas, H.M., Zhu, F-C., Jiang, Y-X., Sun, S-G., Guo, J., Sun, L., Chen, R.: A comparative investigation of metal-suporte interactions on the catalytic activity of Pt nanoparticles for ethanol oxidations in alkaline medium. J. Power Sources 311, 81-90 (2016).

[21] Muench, F., Oezaslan, M., Rauber, M., Kaserer, S., Fuchs, A., Mankel, E., Brötz, J., Strasser, P., Roth, C., Ensinger, W.: Electroless synthesis of nanostructured nickel and nickelboron tubes and their performance as unsupported ethanol electrooxidation catalysts. J. Power Sources 222, 243-252 (2013).

[22] Sun, S., Jusys, Z., Behm, R.J.: Electrooxidation of ethanol on Pt-based and Pd-based catalysts in alkaline electrolyte under fuel cell relevant reaction and transport conditions. J. Power Sources 231, 122–133 (2013).

[23] Geraldes, A.N., da Silva, D.F., Pino, E.S., da Silva, J.C.M., de Souza, R.F.B., Hammer, P., Spinacé, E.V., Neto, A.O., Linardi, M., dos Santos, M.C.: Ethanol electro-oxidation in an alkaline medium using Pd/C, Au/C and PdAu/C electrocatalysts prepared by electron beam irradiation. Electrochim. Acta 111, 455– 465 (2013).

[24] Modibedi, R.M., Masombuka, T., Mathe, M.K.: Carbon supported Pd-Sn and Pd-Ru-Sn nanocatalysts for ethanol electro-oxidation in alkaline medium. Int. J. Hydrogen Energy 36, 4664-4672 (2011).

[25] Antolini, E., Gonzalez, E.R.: Alkaline direct alcohol fuel cells. J. Power Sources 195, 3431–3450 (2010).

[26] Saldan, I., Semenyuk, Y., Marchuk, I., Reshetnyak, O.: Chemical synthesis and application of palladium nanoparticles. J. Mater. Sci 50, 2337–2354 (2015).

[27] Korzec, M., Bartczak, P., Niemczyk, A., Szade, J., Kapkowski, M., Zenderowska, P., Balin, K., Lelatko, J., Polanski, J.: Performance characteristics of air-breathing anion-exchange membrane direct ethanol fuel cells. J. Catal. 313, 1–8 (2014).

[28] Ozturk, Z., Sen, F., Sen, S., Gokagac, G.: The preparation and characterization of nano-sized Pt–Pd/C catalysts and comparison of their superior catalytic activities for methanol and ethanol oxidation. J. Mater. Sci. 47, 8134–8144 (2012).

[29] Hibbitts, D.D., Neurock, M.: Influence of oxygen and pH on the selective oxidation of ethanol on Pd catalysts. J. Catal. 299, 261–271 (2013).

[30] Zalineeva, A., Serov, A., Serov, M. X., Martinez, U., Artyushkova, K., Baranton, S., Coutanceau, C., Atanassov, P.: Nano-structured Pd-Sn catalysts for alcohol electro-oxidation in alkaline medium. Electrochem. Commun. 57, 48–51 (2015).

[31] Liu, F., Zhang, X.B., Haussler, D., Jager, W., Yi, G.F., Cheng, J. P., Tao, X.Y., Luo, Z.Q., Zhou, S.M.: TEM characterization of metal and metal oxide particles supported by multi-wall carbon nanotubes. J. Mater. Sci. 41, 4523–4531 (2006).

[32] Liu, J., Zhou, H., Wang, Q., Zeng, F., Kuang, Y.: Reduced graphene oxide supported palladium–silver bimetallic nanoparticles for ethanol electro-oxidation in alkaline media. J. Mater. Sci. 47, 2188–2194 (2012).

[33] Jou, L.-S., Chang, J.-K., Twhang, T.-J., Sun, I.-W.: Electrodeposition of Palladium–Copper Films from 1-Ethyl-3-methylimidazolium Chloride–Tetrafluoroborate Ionic Liquid on Indium Tin Oxide Electrodes. J. Electrochem. Soc. 156, D193–D197 (2009).

[34] Xu, C., Shen, P.K., Liu, Y.: Ethanol electrooxidation on Pt/C and Pd/C catalysts promoted with oxide. J. Power Sources 164, 527–531 (2007).

[35] Cuña, A., Plascencia, C.R., Leal da Silva, E., Marcuzzo, J., Khan, S., Tancredi, N., Baldan, M.R., Malfatti, C.F.: Electrochemical and spectroelectrochemical analyses of hydrothermal carbon supported nickel electrocatalyst for ethanol electro-oxidation in alkaline medium. Appl. Catal. B 202, 95–103 (2017).

[36] Jongsomjit, S., Prapainainar, P., Sombatmankhong, K.: Synthesis and characterisation of Pd–Ni–Sn electrocatalyst for use in direct ethanol fuel cells. Solid State Ion. 288, 147–153 (2016).

[37] Parreira, L.S., da Silva, J.C.M., D'Villa-Silva, M., Simões, F.C., Garcia, S., Gaubeur, I., Cordeiro, M.A.L., Leite, E.R., dos Santos, M.C.: PtSnNi/C nanoparticle electrocatalysts for the ethanol oxidation reaction: Ni stability study. Electrochim. Acta. 96, 243–252 (2013).

[38] Ciszewski, A., Sron, K., Stepniak, I., Milczarek, G. Nickel(II) lignosulfonate as precursor for the deposition of nickel hydroxide nanoparticles on a glassy carbon electrode for oxidative electrocatalysis. Electrochim. Acta. 134, 355–362 (2014).

[39] Vaithilingam, S., Ramanujam, T. M. Development of rice straw black liquor based porous carbon-poly(aniline-co-methoxy aniline) as supporting for electrochemical performances of alcohol oxidations. Ionics. 24, 3923-3935 (2018).

[40] Zhao, X., Muench, F., Schaefer, S., Brötz, J., Duerrschnabel, M., Molina-Luna, L., Kleebe, H-J., Liu, S., Tan, J., Ensinger, W. Electroless decoration of macroscale foam with nickel nano-spikes: A scalable route toward efficient catalyst electrodes. Electrochem. commun, 65, 39–43 (2016).

[41] Andreuccetti, M.T., Leite, B.S., d´Angelo, J.V.H.: Eucalyptus black liquor – density, viscosity, solids and sodium sulfate contents revisited. O papel 72, 52–57 (2011).

[42] ASTM E1755 - 01(2015) - Standard Test Method for Ash in Biomass.

[43] Brunauer, S., Emmet, P.H., Teller, E.: Adsorption of gases in multimolecular layers. J. Am. Chem. Soc. 60, 309-319 (1938).

[44] Dubinin, M.M.: Fundamentals of the theory of adsorption in micropores of carbon adsorbents: Characteristics of their adsorption properties and microporous structures. Carbon 27, 457-467 (1989).

[45] Gregg, S.J., Sing, K.S.W.: Adsorption: Surface Area and Porosity. Academic Press, London (1982).

[46] Tarazona, P.: Solid-fluid transition and interfaces with density functional approaches. Surf. Sci. 331-333, 989-994 (1995).

[47] Leal da Silva, E., Cuña, A., Khan, S. *et al*. Biomass Derived Carbon as Electrocatalyst Support for Ethanol Oxidation Reaction in Alkaline Medium: Electrochemical and Spectroelectrochemical Characterization. Waste Biomass Valor (2018). https://doi.org/10.1007/s12649-018-0510-8.

[48] Gea, G., Murillo, M. B., Arauzo, J. Thermal Degradation of Alkaline Black Liquor from Straw. Thermogravimetric Study. Ind. Eng. Chem. Res. 41, 4714–4721 (2002).

[49] Sebio-Puñal, T., Naya, S., López-Beceiro, J., Tarrío-Saavedra, J., Artiaga, R. Thermogravimetric analysis of wood, holocellulose, and lignin from five wood species. J. Therm. Anal. Calorim. 109, 1163–1167 (2012).

[50] Tejado, A., Peña, C., Labidi, J., Echeverria, J. M., & Mondragon, I. Physico-chemical characterization of lignins from different sources for use in phenol–formaldehyde resin synthesis. Bioresour. Technol. 98, 1655–1663 (2007).

[51] Alén, R., Rytkönen, S., McKeough, P. Thermogravimetric behavior of black liquors and their organic constituents. J. Anal. Appl. Pyrol. 31, 1–13 (1995).

[52] Pizzi, A.: Advanced Wood Adhesives Technology. Marcel Dekker Inc., New York (1994).

[53] Seo, J., Park, H., Shin, K., Baeck, S.H., Rhym, Y., Shim, S.E.: Lignin-derived macroporous carbon foams prepared by using poly(methyl methacrylate) particles as the template. Carbon. 76, 357-367 (2014).

[54] Arico, E., Tabuti, F., Fonseca, F.C., de Florio, D.Z., Ferlauto, A.S.: Carbothermal reduction of the YSZ–NiO solid oxide fuel cell anode precursor by carbon-based materials. J Therm Anal Calorim. 97, 157–161 (2009).

[55] Lourençon, T.V., Hansel, F.A., da Silva, T.A., Ramos, L.P., de Muniz, G.I.B., Magalhães, W.L.E.: Hardwood and softwood kraft lignins fractionation by simple sequential acid precipitation. Sep. Purif. Technol. 154, 82-88 (2015).

[56] Ibrahim, M.N.M., Zakaria, N., Sipaut, C.S., Sulaiman, O., Hashim, R.: Chemical and thermal properties of lignins from oil palm biomass as a substitute for phenol in a phenol formaldehyde resin production. Carbohydr. Polym. 86, 112-119 (2011).

[57] Celzard, A., Fierro, V., Amaral-Labat, G.: Adsorption by carbon gels Adsorption by Carbons ed J M D Tascon, pp. 205–244. Elsevier, Amsterdam (2012).

[58] Marsh, H., Rodríguez-Reinoso, R.F.: Activated Carbons. Elsevier, Oxford (2006).

[59] Sing, K.S.W., Everett, D.H., Haul, R.A.W., Moscou, L., Pierotti, R.A., Rouquerol, J., Siemienewska, T.: Reporting Physisorption Data for Gas/Solid Systems with Special Reference to the Determination of Surface Area and Porosity. Pure Appl. Chem. 57, 603-619 (1985).

[60] Cuña, A., Tancredi, N., Bussi, J., Deiana, C., Sardella, M.F., Barranco, V., Rojo, J.M.: *E. grandis* as a biocarbons precursor for supercapacitor electrode application. Waste Biomass Valorization 5, 305–313 (2014).

[61] Leal da Silva, E., Ortega Vega, M.R., Correa, P.S., Cuña, A., Tancredi, N., Malfatti, C.F.: Influence of activated carbon porous texture on catalyst activity for ethanol electro-oxidation. Int. J. Hydrogen Energ. 39, 14760-14767 (2014).

[62] Pantea, D., Darmstadt, H., Kaliaguine, S., Roy, C.: Electrical conductivity of conductive carbon blacks: influence of surface chemistry and topology. Applied Surface Science 217, 181–193 (2003).

[63] Goula, M.A., Charisiou, N.D., Papageridis, K.N., Delimitis, A., Pachatouridou, E., Iliopoulou, E.F.: Nickel on alumina catalysts for the production of hydrogen rich mixtures via the biogas dry reforming reaction: Influence of the synthesis method. Int. J. Hydrogen Energy 40, 9183-9200 (2015).

[64] Xu, C., Hu, Y., Rong, J., Jiang, S.P., Liu, Y.: Ni hollow spheres as catalysts for methanol and ethanol electrooxidation. Electrochem. Comm. 9, 2009–2012 (2007).

[65] Wicklein, B., Arranz, J., Mayoral, A., Aranda, P., Huttel, Y., Ruiz-Hitzky, E.: Nanostructured carbon–metal hybrid aerogels from bacterial cellulose. RSC Adv. 7, 42203-42210 (2017).

[66] Jiang, L., Yan, J., Hao, L., Xue, R., Sun, G., Yi, B.: High rate performance activated carbons prepared from ginkgo shells for electrochemical supercapacitors. Carbon 56, 146 – 154 (2013).

[67] Moreno-Castilla, C., Lopez-Ramon, M.V., Carrasco-Marin, F.: Changes in surface chemistry of activated carbons by wet oxidation. Carbon 38, 1995– 2001 (2000).

[68] Biniak, S., Szymanski, G., Siedlewski, J., Swiatkowski, A.: The characterization of activated carbons with oxygen and nitrogen surface groups. Carbon 35, 1799–1810 (1997).

[69] Bandosz, T.J., Ania, C.O.: Surface chemistry of activated carbons and its characterization, in: T.J. Bandosz (Ed.), Activated Carbon Surfaces in Environmental Remediation, pp. 159–229. Elsevier, New York (2006).

[70] Xing, W., Qiao, S., Wu, X., Gao, X., Zhou, J., Zhuo, S., Hartono, S.B., Hulicova-Jurcakova, D.: Exaggerated capacitance using electrochemically active nickel foam as current collector in electrochemical measurement. J. Power Sources, 196, 4123–4127 (2011).

[71] Dutta, A., Adhikary, R., Broekmann, P., Datta, J.: Intelligent catalytic support by Ni / NiO / Ni(OH)2 in low level of Pd/Pt boosting the performance of alkaline DEFC. Appl. Catal. B-Environ. 257, 117847 (2019).

[72] Ureta-Zañartu, M.S., Berríos, C., Pavez, J., Zagal, J., Gutiérrez, C., Marco, J.F.: Electrooxidation of 2-chlorophenol on polyNiTSPc-modified glassy carbon electrodes. J. Electroanal. Chem. 553, 147-156 (2003).

[73] Castro, C., Millan A., Palacio F.: Nickel oxide magnetic nanocomposites in an imine polymer matrix. J. Mater. Chem. 10, 1945-1947 (2000).

[74]Zhang, X., Shi, W., Zhu, J., Zhao, W., Ma, J., Mhaisalkar, S., Maria, T.L., Yang, Y., Zhang, H., Hng, H.H., Yan, Q.: Synthesis of Porous NiO Nanocrystals with Controllable Surface Area and Their Application as Supercapacitor Electrodes. Nano Res. 3, 643–652 (2010).

[75] Song, P., Wen, D., Guo, Z. X., Korakianitis, T.: Oxidation investigation of nickel nanoparticles. Phys. Chem. Chem. Phys. 10, 5057–5065 (2008).

[76] Compton R. G. and Banks C. E.: Understanding Voltammetry. Imperial College Press, London (2011).

[77] Fleischmann, M., Korinek, K., Pletcher, D.: The oxidation of organic compounds at a nickel anode in alkaline solution. J. Electroanal. Chem. Interfacial Electrochem. 31, 39-49 (1971).

[78] Zhan, J., Cai, M., Zhang, C., Wang, C.: Synthesis of mesoporous $NiCo_2O_4$ fibers and their electrocatalytic activity on direct oxidation of ethanol in alkaline media. Electrochim. Acta 154, 70–76
(2015).

[79] Sheikh, A.M., Correa, P.S., Leal da Silva, E., Savaris, I.D., Amico, S.C., Malfatti, C.F.: Energy conversion using Pd-based catalysts in direct ethanol fuel cell. Renewable Energy and Power Quality Journal 1 (11), 342-345 (2013).

[80] Shen, S.Y., Zhao, T.S., Xu, J.B., Li, Y.S.: Synthesis of PdNi catalysts for the oxidation of ethanol in alkaline direct ethanol fuel cells. J. Power Sources 195, 1001-1006 (2010).

[81] Gupta, U.K., Pramanik, H.: Electrooxidation study of pure ethanol/methanol and their mixture for the application in direct alcohol alkaline fuel cells (DAAFCs). Int. J. Hydrog. Energia 44, 421-435 (2019).

[82] Carlson, G., Lewis, D., McKinley, K., Richardson, J. Tillotson T.: Aerogel commercialization: technology, markets and costs. J. Non-Cryst Solids 186, 372–379 (1995).